Available online at www.sciencedirect.com

SciVerse ScienceDirect

Ceramics International 38 (2012) 5853–5857

CERAMICS INTERNATIONAL

www.elsevier.com/locate/ceramint

Microstructural design of $BaTiO_3$-based ceramics for temperature-stable multilayer ceramic capacitors

Jing Wang [a,b,*], Shenglin Jiang [a], Dan Jiang [b], Jiajia Tian [b], Yunlong Li [b], Yue Wang [b]

[a] Department of Electronic Science and Technology, Huazhong University of Science and Technology, Wuhan 430074, China
[b] College of Chemistry and Environmental Science, HeBei University, Baoding 71002, China

Received 6 March 2012; received in revised form 11 April 2012; accepted 11 April 2012
Available online 19 April 2012

Abstract

In order to satisfy EIA X8R specification, a new type of $BaTiO_3$-based ceramic with hierarchical structure in a formula scheme "a ferroelectric ABO_3 + another ferroelectric ABO_3", was designed. There were (Ba, Bi)TiO_3 and Ba(Ti, Zr)O_3 phases with different Curie temperatures coexisting in the grains from inside to outside, prepared by wet chemical method under 100 °C. The hierarchical structure of the ceramic grains was proved by X-ray diffraction (XRD), scanning electron microscopy (SEM) and energy dispersive X-ray spectroscopy (EDX). The dielectric constant of (Ba, Bi)TiO_3–Ba(Ti, Zr)O_3 ceramic was ~6000, the $\Delta C/C_{20\,^\circ C}$ was −12.0%, 14.1%, and −8.3% at −55 °C, 130 °C, and 160 °C, respectively, and the dielectric loss is less than 0.1, which is obviously superior to (Ba, Bi)TiO_3 and Ba(Ti, Zr)O_3. The results of this work showed that the formula scheme "a ferroelectric ABO_3 + another ferroelectric ABO_3" for solid solutions is a promising approach to prepare high performance temperature-stable capacitor materials.

PACS : 77.84.Cg

Keywords: Temperature-stability; Dielectric ceramic; $BaTiO_3$-baced solid solution; Hierarchical structure

1. Introduction

Multilayer ceramic capacitors (MLCCs) are one of the most important electronic components because of their economical volumetric efficiency for capacitance and high reliability. High performance MLCCs require high dielectric constant and good stability as the market drives electronic devices toward ever-greater miniaturization and multifunctionality [1]. Due to the potential applications in a wide range of electronic devices, such as multilayer ceramic capacitors, transducers, infrared detectors, and pulse generating devices [2,3], the crystal structure, ferroelectric phase transition, dielectric properties of $BaTiO_3$ and related $BaTiO_3$-based ceramics have been extensively investigated. Many studies have been carried out to investigate the dielectric temperature-stability of $BaTiO_3$ ceramic in a comparatively wide temperature rage [4–6], because electronic parts in the control module for automotive uses must keep their performance under high temperature [7]. Many $BaTiO_3$-based X7R multilayer ceramic capacitors (MLCCs) have been widely used for miniaturization of electronic components attributed to their temperature-stable dielectric behavior, namely the variation of capacity ($\Delta C/C_{20\,^\circ C}$) less than ±15% over the temperature range from −55 to 125 °C (upper working temperature 125 °C). However, there is increasing need to extend the working range of these devices to 150 °C to achieve X8R specification [8].

Pure $BaTiO_3$ is a ferroelectric perovskite (ABO_3) with a high room temperature permittivity (~2000–3000) and a modest Curie temperature, $T_C \sim 130\,^\circ C$ [4]. When temperature is higher than 130 °C, the permittivity will drop dramatically so that the material cannot be used sequentially at this temperature. At this time, the temperature dependence of capacitance change illustrates the so-called "clockwise effect" [9]. The growing trend is to reduce dielectric thickness and increased stacking of electrode layers to meet miniaturization of electronic components [10]. However, the clockwise effect

* Corresponding author at: Department of Electronic Science and Technology, Huazhong University of Science and Technology, Wuhan 430074, China. Tel.: +86 312 5079359; fax: +86 312 5079505.
E-mail addresses: wangjing9804@163.com (J. Wang), jsl@mail.hust.edu.cn (S. Jiang).

0272-8842/$36.00
http://dx.doi.org/10.1016/j.ceramint.2012.04.036

will be remarkable with the reduced thickness, namely the dielectric properties of MLCC will be exacerbated at the temperature higher than 130 °C [11]. Thus extending the range of $BaTiO_3$ ceramic usage scope to high temperature is essential to realize X8R MLCC materials.

In order to improve the temperature coefficient of $BaTiO_3$, various works have been focused on the preparation of the $BaTiO_3$-based ceramic powder with core–shell structure by the traditional solid-phase method, through adulteration of chemical nonuniformity, e.g. mixing $BaTiO_3$ powder with some oxidates, such as rare earth oxidates, Nb_2O_5, Co_2O_3, and Bi_2O_3 [12,13]. Namely, the ceramic crystal is comprised of two parts: pure $BaTiO_3$ as grain core (ferroelectric tetragonal phase) and oxidate-doped $BaTiO_3$ as grain shell (paraelectric cubic phase), with the transition region between the core and the shell [14]. However, the dielectric constant of barium titanate-based ceramic materials is greatly dependent on the ferroelectric tetragonal phase. It is well-known that the permittivity of $BaTiO_3$ capacitor will decrease remarkably when it is turned from the ferroelectric tetragonal phase into paraelectric cubic phase. Recently, bismuth-based dielectric ceramics have been broadly studied for its relatively low sintering temperature (less than 1000 °C), high dielectric constant and have been investigated for the application as multilayer capacitors [15,16]. Zr^{4+} modified $BaTiO_3$ ceramic exhibits a high dielectric constant, a low dissipation and ability to shift T_C to a low temperature [17–19].

In this paper, we reported a new structure type of $BaTiO_3$ ceramic crystal with hierarchical structure. The crystal grain consists of several $BaTiO_3$-based phases with different chemical compositions in a formula scheme ''a ferroelectric ABO_3 + another ferroelectric ABO_3'', from inside to outside. Each phase has specific Curie temperature and Curie peak, according to different dopants prepared by wet chemical method. There are two Curie peaks at high-temperature region and low-temperature region, respectively in the whole scope of working temperature. The temperature stability will be greatly improved after multiplying of those Curie peaks, presenting multi-peak effect. Meanwhile, the permittivity of the material can maintain a high level by choosing proper doping elements. This enables extensive tailoring of their dielectric properties by choosing an appropriate $BaTiO_3$-based phase with specific T_C and dielectric constant. In the present investigation, $(Ba_{0.985}Bi_{0.01})TiO_3$–$Ba(Ti_{0.9}Zr_{0.1})O_3$ (abbreviated BBT–BTZ) powder and ceramic were synthesized, and the microstructures and dielectric properties of $(Ba_{0.985}Bi_{0.01})TiO_3$–$Ba(Ti_{0.9}Zr_{0.1})O_3$ ceramics were thus measured. $(Ba_{0.985}Bi_{0.01})TiO_3$ (BBT) and $Ba(Ti_{0.9}Zr_{0.1})O_3$ (BTZ) ceramic were also prepared for contrast examinations.

2. Experimental procedure

2.1. Preparation of BBT powder

The BBT powder studied was prepared using liquid-state method with Bi_2O_3, $TiCl_4$ and $Ba(OH)_2{\cdot}8H_2O$ (AR 99.0% China) as raw materials. Firstly, $TiCl_4$ was hydrolyzed in stoichiometric Bi_2O_3 hydrochloric acid solution to form a transparent solution. Then $Ba(OH)_2{\cdot}8H_2O$ was dissolved in boiling water and mixed with the above solution in a flask to form a homogeneous solution. Secondly, the mixture was heated to 95–100 °C by a heating jacket with vigorous and continuous stirring for 4 h. The reaction product then was obtained after washing and drying in the air.

2.2. Preparation of BBT–BTZ powder

$ZrOCl_4{\cdot}8H_2O$, $TiCl_4$, $Ba(OH)_2{\cdot}8H_2O$ (AR 99.0% China) and the aforementioned BBT were used as starting materials. Firstly, $TiCl_4$ was hydrolyzed in stoichiometric $ZrOCl_4$ hydrochloric acid solution, and mixed with $Ba(OH)_2$ boiling water solution in a flask to form a homogeneous solution by stirring. Secondly, BBT was put into the three-necked flask and mixed with the solution together, reacted in 95–100 °C for 4 h. Then BTZ would grow at the surface of BBT, because the similarity of their geometrical structure enabled BBT as seed crystal to induce the growth of BTZ on the surface. It will be proved by the following characterizations.

2.3. Preparation of BBT–BTZ ceramics

The prepared ceramic powders were pressed in disk form (20 mm in diameter and 2 mm in thickness) using 8 wt% of PVA as a binder. After discharging binder, the disks were finally fired at 1100 °C for 1 h in air. Silver paste was fired on both sides of the samples at 550 °C for 10 min as electrodes.

Dielectric measurements of the samples were performed by using a LCR meter at 1 kHz in the temperature range from −55 °C to 180 °C. Phase analysis is carried out by X-ray diffraction (XRD) technique using the Cu Kα radiation of D8 Advance. Scanning electron micrographs (SEM) is recorded with a Jeol 940A electron microscope. A point-to-point nano-analysis has been done using scanning transmission electron microscope (STEM) with energy dispersive X-ray spectroscopy (EDX) facility.

3. Results and discussion

Fig. 1 shows the XRD patterns for all the doped $BaTiO_3$ compositions of BTZ, BBT, and BBT–BTZ. These XRD patterns were measured on the sintered ceramic pellets. There was no trace of secondary peak in BTZ and BBT patterns (Fig. 1a and b), which suggests the formation of homogeneous solid solution with perovskite phase. It is evident that XRD peaks of BBT shift to a large angle, which indicates the decrease of lattice parameters. It is due to the radius of Bi^{3+} (0.103 nm) smaller than that of Ba^{2+} (0.135 nm), which occupies Ba-site. Instead, the XRD peaks of BTZ shift toward small angle, which is attributed that the radius of Zr^{4+} (0.072 nm) is larger than that of Ti^{4+} (0.060 nm). The ionic radii used are those of Shannon [20,21]. However, BBT–BTZ shows two peaks in each peak position, which belongs to BBT and BTZ, respectively according to the relative shift to the peak position of pure $BaTiO_3$. It is observed obviously in Fig. 2. This

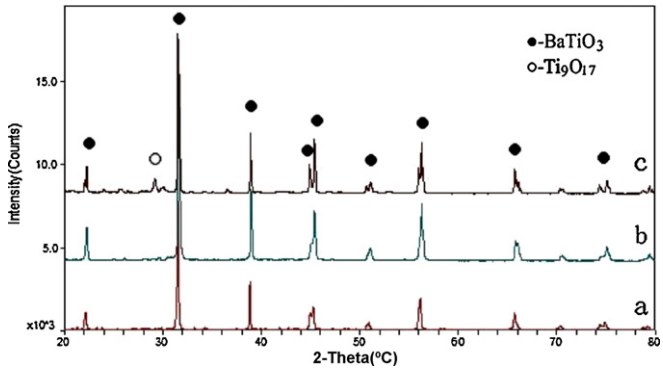

Fig. 1. XRD patterns of $BaTiO_3$-based ceramic: (a) BTZ, (b) BBT, and (c) BBT–BTZ.

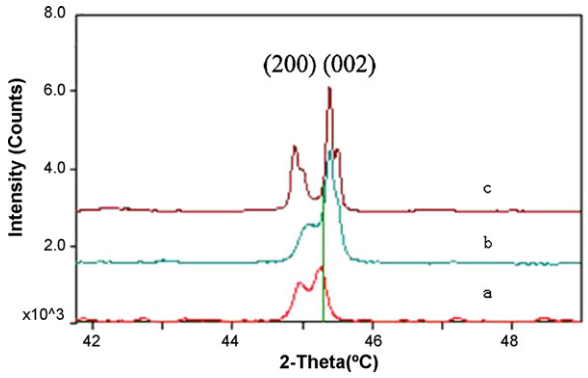

Fig. 2. XRD peaks at $2\theta = 45.294^\circ$ of (a) BTZ, (b) BBT, and (c) BBT–BTZ (the vertical line represents the peak position of pure $BaTiO_3$).

result indicates there are two different phases of BBT and BTZ coexisting in BBT–BTZ ceramic. The secondary phase is observed by XRD in BBT–BTZ, which is proved to be Ti_9O_{17}. The reasons for the emergence of Ti_9O_{17} will be discussed in another paper. The *c*/*a* ratio and volume of the unit cell were calculated, shown in Table 1.

The (0 0 2) and (2 0 0) diffraction peaks of the $BaTiO_3$ solid solution for the determination of the crystal system are shown in Fig. 2. The (0 0 2) and (2 0 0) diffraction lines are separated from each other with the addition of Bi, Zr, which suggests BBT and BTZ exhibited tetragonal structure.

Table 1
The *c*/*a* ratio and unit cell volume of BBT, BTZ and BBT–BTZ.

Sample	BBT	BTZ	BBT–BTZ
c/*a* ratio	1.000577	1.000684	1.008771
Unit cell volume (nm^3)	64.07478	64.5753	64.31962

Table 2
Dielectric properties of BBT, BTZ and BBT–BTZ.

Temperature (°C)	Dielectric constant			Dielectric loss of BBT–BTZ
	BBT	BTZ	BBT–BTZ	
−55	946	1435	4501	0.01
−40	985	1500	4700	0.01
−20	1000	1745	4803	0.016
0	1022	1821	4871	0.032
20	1025	2139	5117	0.055
40	1038	2778	5439	0.082
60	1123	2971	5669	0.093
80	1263	2818	5744	0.039
100	1530	2443	5546	0.031
120	2254	2028	5723	0.02
140	2758	1749	5482	0.03
160	2102	1521	4688	0.013

The relative density of BBT and BBT–BTZ pellets sintered at 1100 °C are ∼95–98%, which shows good sintering properties. Fig. 3a is the SEM photo of BBT, with an average grain size of 300 nm. Fig. 3b is the SEM photo of BBT–BTZ, with an average grain size of ∼1 μm. There is no secondary phase detected in both photos. Considering the XRD pattern of BBT–BTZ in which BBT and BTZ coexist (the content of Ti_9O_{17} is too little to be calculated), it is believed that BTZ is grown on the BBT surface to form hierarchical structure.

Fig. 4 illustrates STEM/EDX point-to-point analyses across the diameter of grain for BBT–BTZ. The result suggests that the content of Bi^{3+} is higher and the content of Zr^{4+} is lower at the grain core than that of those at grain shell, which indicates that BBT is coated by BTZ. The results are in good agreement with XRD and SEM.

The dielectric constant and dissipation data of BBT, BTZ and BBT–BTZ samples are shown in Table 2. The maximum

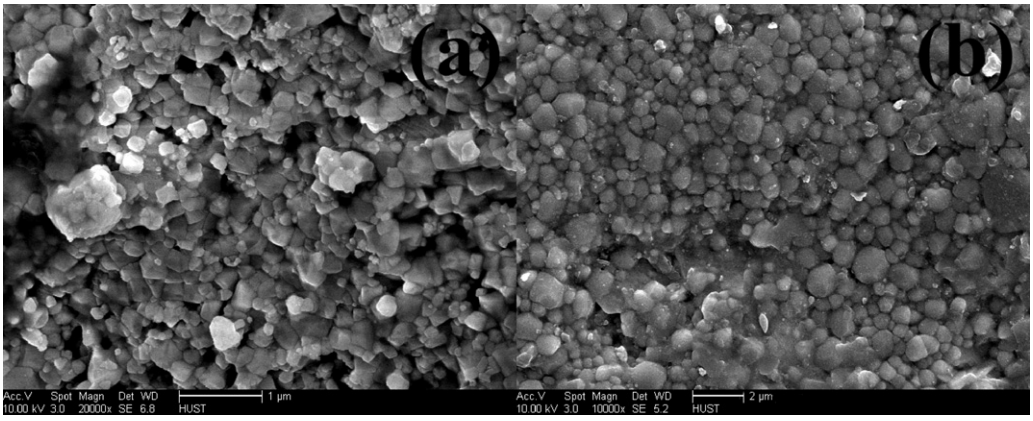

Fig. 3. SEM photos of (a) BBT and (b) BBT–BTZ.

dielectric constant is up to ~6000 and dissipation is less than 0.1. Fig. 5 depicts the temperature dependences of capacitance change (ε–T curve) of BBT, BTZ, BBT–BTZ samples, while the fitting curve of BBT and BTZ (nominated as fitting-BBT–BTZ) is drawn for comparison. As the figure shows, addition of Zr element to $BaTiO_3$ gives a movement of T_C to low temperature of 60 °C. As Kell and Hellicar [22] indicated, the substitution of Ti^{4+} ions by Zr^{4+} ions leads to a reduction in Curie temperature for $BaTiO_3$-based ceramics. However, the addition of Bi gives a movement to high temperature of 135 °C. The curve of fitting-BBT–BTZ describes the possible temperature dependence of capacitance change of BBT–BTZ calculated from volume percent and dielectric constant using Lichnetecker law. However, the actual BBT–BTZ ε–T curve shows a high dielectric constant and stability that disagrees with the fitting curve shown in Fig. 6. This result may be ascribed to the tension between the two phases. During sintering, internal tension comes into being because the two phases have different coefficients of thermal expansion. The internal tension promotes the tetragonal distortion, which is associated closely with permittivity. The dielectric constant rises with the increase of tetragonality (*c*/*a* ratio). The *c*/*a* ratio of BBT–BTZ is larger obviously than those of BBT and BTZ, shown in Table 1 and that can explain the high permittivity of BBT–BTZ qualitatively. High stability is due to the diffusion of the two phases into each other, which always induces dielectric peaks broadening.

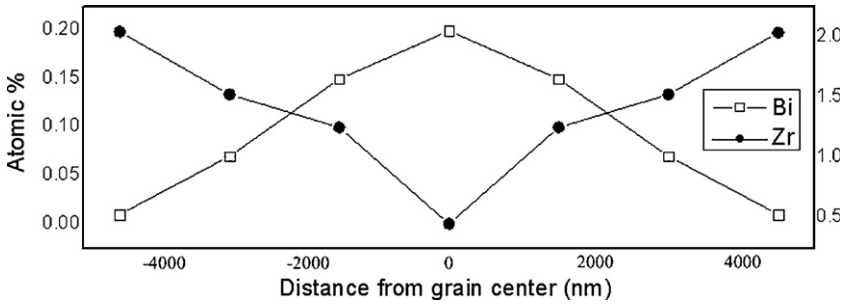

Fig. 4. EDX composition profile across the diameter of grain for BBT–BTZ sample.

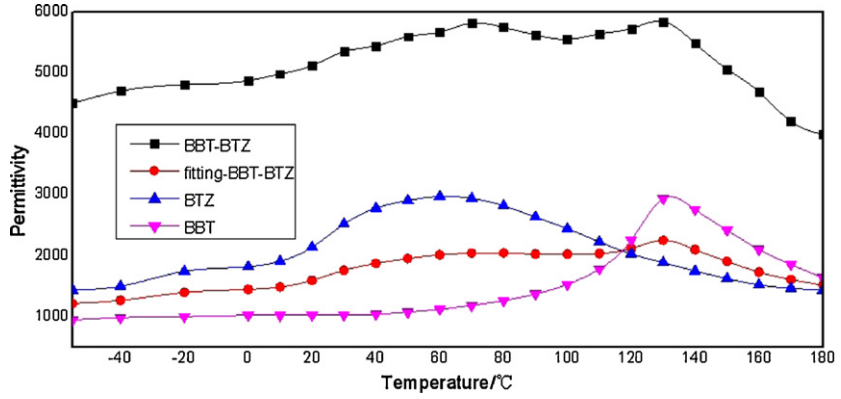

Fig. 5. Temperature dependence of capacitance change of BaTiO3-baced ceramic and the fitting of BBT and BTZ.

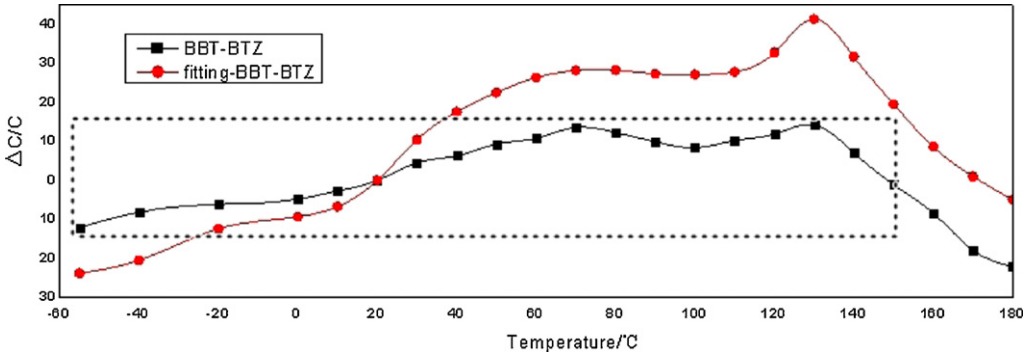

Fig. 6. Temperature coefficient of capacitance (TCC) of BBT–BTZ ceramic and fitting-BBT–BTZ.

4. Conclusions

1. A new type of $BaTiO_3$-based ceramic with hierarchical structure was designed. There were (Ba, Bi)TiO_3 and Ba(Ti, Zr)O_3 phases with different T_C coexisting in the ceramic grains from inside to outside. The phase composition is proved by XRD patterns, SEM photos and EDX profile. This demonstrates a promising avenue in the search for high performance capacitor materials with temperature-stability in the formula scheme "a ferroelectric ABO_3 + another ferroelectric ABO_3".
2. Hierarchical structure ceramic for X8R MLCC was prepared from (Ba, Bi)TiO_3–Ba(Ti, Zr)O_3 powder, which is synthesized by wet chemical method under 100 °C. This method is simple, effective, low cost and easy maneuverability.
3. The dielectric constant and stability of (Ba, Bi)TiO_3–Ba(Ti, Zr)O_3 ceramic is obviously superior to (Ba, Bi)TiO_3 and Ba(Ti, Zr)O_3. The dielectric properties are: $\varepsilon = \sim 6000$, $\Delta C/C_{20\,^\circ C}$ is -12.0%, 14.1, and -8.3% at -55, 130, and 160 °C, respectively, dielectric loss is less than 0.1.

Acknowledgements

This work is funded by Graduates' Innovation Fund of Huazhong University of Science and Technology (contract HF07042010185) and Youth Fund of Hebei University (contract 2008Q23).

References

[1] T.A. Jain, K.Z. Fung, S. Hsiao, J. Chan, Effects of BaO–SiO_2 glass particle size on the microstructures and dielectric properties of Mn-doped Ba(Ti Zr)O_3 ceramics, Journal of the European Ceramic Society 30 (2010) 1469–1476.

[2] P.S. Dobal, A. Dixit, R.S. Katiyar, Z. Yu, R. Guo, A.S. Bhalla, Micro-Raman scattering and dielectric investigations of phase transition behavior in the $BaTiO_3$–$BaZrO_3$ system, Journal of Applied Physics 89 (2001) 8085–8091.

[3] N. Baskaran, A. Ghule, C. Bhongale, R. Murugan, H. Chang, Phase transformation studies of ceramic $BaTiO_3$ using thermo-Raman and dielectric constant measurements, Journal of Applied Physics 91 (2002) 10038–10043.

[4] L. Zhang, O.P. Thakur, A. Feteira, G.M. Keith, A.G. Mould, D.C. Sinclair, A.R. West, Comment on the use of calcium as a dopant in X8R $BaTiO_3$-based ceramics, Applied Physics Letters 90 (2007) 142914.

[5] L.X. Li, Y.M. Han, P. Zhang, C. Ming, X. Wei, Synthesis and characterization of $BaTiO_3$-based X9R ceramics, Journal of Materials Science 44 (2009) 5563–5568.

[6] E.S. Na, S.C. Choi, U. Paik, Temperature dependence of dielectric properties of rare-earth element doped $BaTiO_3$, Journal of Ceramic Processing Research 4 (2003) 181–184.

[7] Y.S. Jung, E.S. Na, U. Paik, A study on the phase transition and characteristics of rare earth elements doped $BaTiO_3$, Materials Research Bulletin 37 (2002) 1633–1640.

[8] H. Kishi, Y. Mizuno, H. Chazono, Base-metal electrode-multilayer ceramic capacitors: past present and future perspectives, Japanese Journal of Applied Physics 42 (2003) 1–15.

[9] B. Tang, S.R. Zhang, X.H. Zhou, Y. Yuan, Doping effects of Mn^{2+} on the dielectric properties of glass-doped $BaTiO_3$-based X8R materials, Journal of Materials Science-Materials in Electronics 18 (2007) 541–545.

[10] Y. Mizuno, T. Hagiwara, H. Kishi, Microstructural design of dielectrics for Ni-MLCC with ultra-thin active layers, Journal of the Ceramic Society of Japan 115 (2007) 360–364.

[11] H. Kobayashi, Dielectric ceramic composition and electronic device TDK Corporation (Tokyo JP), United States Patent, 2002.

[12] K.J. Park, C.H. Kim, Y.J. Yoon, S.M. Song, Y.T. Kim, K.H. Hur, Doping behaviors of dysprosium yttrium and holmium in $BaTiO_3$ ceramics, Journal of the European Ceramic Society 29 (2009) 1735–1741.

[13] H.I. Hsiang, L.T. Mei, Y.J. Chun, Dielectric properties and microstructure of Nb–Co codoped $BaTiO_3$–$(Bi_{0.5}Na_{0.5})TiO_3$ ceramics, Journal of the American Ceramic Society 92 (2009) 2768–2771.

[14] R.Z. Chen, X.H. Wang, Z.L. Gui, L.T. Li, Effect of silver addition on the dielectric properties of barium titanate-based X7R ceramics, Journal of the American Ceramic Society 86 (2003) 1022–1024.

[15] H.C. Ling, M.F. Yan, W.W. Rhodes, High dielectric constant and small temperature coefficient bismuth-based dielectric compositions, Journal of Materials Research 5 (1990) 1752–1762.

[16] D.H. Liu, Y. Liu, S.Q. Huang, X. Yao, Phase structure and dielectric properties of Bi_2O_3–ZnO–Nb_2O_3-based dielectric ceramics, Journal of the American Ceramic Society 76 (1993) 2129–2132.

[17] S.M. Neirman, The curie point temperature of $Ba(Ti_{1-x}Zr_x)O_3$ solid solutions, Journal of Materials Science 23 (1988) 3973–3980.

[18] E. Antonelli, R.S. Silva, A.C. Hernandes, $Ba(Ti_{1-x}Zr_x)O_3$ ($x = 0.05$ and 0.08) ceramics obtained from nanometric powders: ferroelectric and dielectric properties, Ferroelectrics 75 (2006) 351–358.

[19] C.E. Ciomaga, M.T. Buscaglia, V. Buscaglia, L. Mitoseriu, Oxygen deficiency and grain boundary-related giant relaxation in Ba(Zr,Ti)O_3 ceramics, Journal of Applied Physics 110 (2011) 114110.

[20] R.D. Shannon, Empirical electronic polarizabilities in oxides, hydroxides, oxyfluorides, and oxychlorides, Physical Review B 73 (2006) 235111.

[21] R.D. Shannon, Dielectric polarizabilities of ions in oxides and fluorides, Journal of Applied Physics 73 (1993) 348–366.

[22] R.C. Kell, N.J. Hellicar, Structure transitions in barium titanate zirconate transducer materials, Acustica 6 (1956) 235–238.